J Solid State Electrochem (1999) 3: 446–456

ORIGINAL PAPER

Bineta Keita · Essadik Abdeljalil · François Girard
Sophie Gerschwiler · Louis Nadjo
Roland Contant · Christian Haut

Electrochemically induced transformations of heteropolyanions: new electroactive metal oxide films studied by the electrochemical quartz crystal microbalance

Received: 2 December 1998 / Accepted: 26 January 1999

Abstract New oxide films have been electrodeposited from $[P_2Mo_{18}O_{62}]^{6-}$ by potential cycling in mildly acidic aqueous media. To obtain an adherent and persistent film, it is necessary that more than six electrons/molecule be fixed on the framework of the heteropolyanion. The film is then studied in pure supporting electrolyte. In this medium, a remarkable current increase is observed during the potential cycling. Whether the film is deposited on a glassy carbon electrode or on the gold electrode of an electrochemical quartz crystal microbalance (EQCM), exactly the same steady current increase up to a maximum is obtained in cyclic voltammetric measurements. The EQCM reveals a steady mass increase during the continuous cycling of the film in the supporting electrolyte. This behaviour is interpreted as featuring an irreversible water and electrolyte intake into the film, up to a maximum, after which the phenomena observed during reduction and oxidation processes are taken as featuring intercalation/deintercalation, respectively. This behaviour is much the same as described in the literature for WO_3 and MoO_3 bronzes, except that the present films seem very stable and have shown no tendency to dissolve or deactivate.

Key words Heteropolyanion · Metal oxides · Intercalation/deintercalation · Electrochemical quartz crystal microbalance · Cyclic voltammetry

B. Keita · E. Abdeljalil · F. Girard · S. Gerschwiler · L. Nadjo (✉)
Laboratoire de Physicochimie des Rayonnements,
Associé au CNRS, Electrochimie et Photoélectrochimie,
Université Paris-Sud, Bâtiment 420, F-91405 Orsay Cedex, France
e-mail: nadjo@icmo.u-psud.fr

R. Contant
Laboratoire de Chimie des Métaux de Transition,
Associé au CNRS, Université Paris VI, 4 place Jussieu,
F-75252 Paris Cedex 05, France

C. Haut
Laboratoire de Métallurgie Structurale,
Associé au CNRS, Université Paris-Sud, Bâtiment 415,
F-91405 Orsay Cedex, France

Introduction

Electrochemistry studies, from our group and from others, have largely demonstrated the existence of catalytic properties for oxometalates toward numerous chemicals in solution [1–7]. We have performed extensive studies on proton, nitrite and nitric oxide reduction or NADH oxidation. These studies were based on unambiguous cyclic voltammetry and preparative scale electrolysis experiments. Problems remaining to be solved concern nitrite and nitric oxide and include, in particular, the identification and quantification of the products obtained by preparative electrolysis at the potentials of the catalytic waves, and the mechanistic pathways through which the catalysis proceeds. In this direction, the work by Toth and Anson [4] deserves emphasis: these authors also demonstrated that Keggin-type iron-substituted polyoxometalates catalyze the reduction of nitrite and nitric oxide; the reduction occurs primarily through the formation of an iron nitrosyl complex that is further reduced at more negative potentials by electrons accumulated in the tungsten framework. The product obtained was ammonia, with a relatively poor yield [4]. The authors presume that this result might be due, at the potential necessary to accumulate the right number of electrons, to the electrode derivatization discovered previously and studied in some detail by our group [8–14]. Recently, we have shown that a series of one- and two-electron reduced heteropolyanions of the Keggin and Dawson series convert *quantitatively* NO into N_2O in acidic aqueous media [15]. Unsubstituted and lacunary heteropolyanions, as well as the heterometal-substituted heteropolyanions of these two groups, prove active for this purpose.

One of our aims in the catalytic and electrocatalytic use of oxometalates is to build stable modified catalytic electrodes useful for the easy synthesis of measurable amounts of chemicals. The results obtained, thus far, first with the oxometalate in solution, and then with the oxometalate entrapped in polymer matrices [3], are

rather satisfactory. Direct electrodeposition of heteropolyanions in mild conditions on electrodes should also give catalytic surfaces.

With this reasoning and all the preceding results in mind, our group is developing work on oxometalates in several complementary directions, two of which are briefly summarized in the following:

- To catalyse reactions that need several electrons to be performed, it is interesting to avoid driving the working electrode potential to too negative values, while increasing the yield of these favourable reactions; then, we set out to synthesize heteropolyanions which could accumulate, in suitable media, several electrons on their first wave or on their first of several rather positive waves [16]. It is expected that better selectivity and enhanced synthesis yields will ensue.
- It is necessary to try and transfer the catalytic activity observed in solution to electrode surfaces. Use of polymer matrices or, particularly, direct electrodeposition of oxometalates are not easy tasks. We have already demonstrated that the catalysts electrodeposited at −1.2 V vs. SCE in acid medium and active for the hydrogen evolution reaction do not necessarily keep the Keggin or Dawson structure of the starting heteropolyanion. Then, our strategy of stepwise variation of the potential of the working electrode for the electrodeposition [17] seems appropriate, in order to obtain a better insight into the significance of the observations made at each step. Very recently, our group has confirmed the interest of this approach [18]. It has been demonstrated that composite films of new electroactive metal oxides can be electrodeposited on electrode surfaces in very mild pH and potential conditions. The appropriate starting substances were molybdenum-substituted tungsten frameworks and fully molybdic compounds. Not unexpectedly, the results show the existence of different new species depending on the specific starting oxometalate [18]. Hence, the idea is that we might be synthesizing new families of substances and opening up the way to complex, specific (hopefully) catalytic decomposition and/or polymerization products of the heteropolyanions. As a matter of fact, we and others have now established that [W^{VI}, W^{V}] or [Mo^{VI}, Mo^{V}] mixtures are useful catalysts and electrocatalysts [8, 9 (and references therein), 19–21].

During the study of such films in pure supporting electrolyte, a puzzling observation was made: upon continuous cycling of several such films, a steady current increase is observed, which is a function of time and also of the number of cycles. In an attempt to understand this behaviour, the present paper is mainly devoted to an electrochemical quartz crystal microbalance (EQCM) study of the electrodeposition, growth and electrochemical behaviour of such films. We focus on $[P_2Mo_{18}O_{62}]^{6-}$, which is one of the representative oxometalates in the catalytic and quantitative reduction of NO to N_2O [15]. The EQCM technique is particularly useful in related studies [22 (and references therein)]. For instance, we and others [23, 24] have demonstrated previously, with this technique, that the oxidized form of heteropolyanions adsorbs on electrode surfaces. Owing to their numerous catalytic properties, the adsorbability of oxometalates on various materials has been largely studied by a variety of techniques [17, 25–32, 33 (and references therein)]. The EQCM, however, has some specific possibilities: it has permitted us to estimate easily the deposited amounts of a substance, and to monitor the influence of several parameters including the supporting electrolyte composition, the polyanion concentration, etc., on the adsorption kinetics. In the following, the EQCM also proved useful for the study of the charge transport kinetics within the deposited films. Several such features are unique to EQCM studies.

Experimental

Apparatus and experimental set-up

The reference electrode was a saturated calomel electrode (SCE), the counter electrode a platinum gauze of large surface area. These electrodes were kept in compartments containing the appropriate supporting electrolyte and separated from the working electrode compartment by a medium-porosity glass frit for the counter electrode, and a fine-porosity ceramic frit for the reference electrode. The EQCM set-up used in this work was the system QCA 917 (Seiko/EG&G) using 9-MHz AT-cut crystals with gold electrodes. Prior to each experiment, the gold electrodes were handled as described previously [23]. Calibration of the QCM had been performed as described previously [23] using silver electrodeposition under potentiostatic conditions. The calibration constant was $K = 0.730$ Hz ng^{-1} for the Seiko/EG&G system. It was in agreement with the value expected for the 9-MHz AT-cut quartz crystals. The handling of other electrodes not coupled to the EQCM has been described previously [13].

Preliminary scanning electron microscopy (SEM) experiments were performed on a LEO 260 microscope equipped with energy-dispersive spectroscopy comprising a detector with a thin window (NORAN Instruments) complemented with a ROENTEK system for quantitative analysis.

The electrochemical set-up was an EG&G 273 A potentiostat driven by a PC with the 270 software. The data from the Seiko/EG&G system were recorded in the computer and then printed, when necessary, on an HP Deskjet 560 C printer.

In the present study, we explore electrodeposition by potential cyclic voltammetry. We found that potentiostatic conditions can also be used to obtain film electrodeposition on the electrode surface. The corresponding results will be published elsewhere.

Chemicals

Pure water was used throughout. It was obtained by passing water through a Milli RO4 unit and subsequently through a Millipore Q water purification set. All the chemicals were of high purity grade and were used as received. H_2SO_4 and Na_2SO_4 (Prolabo) were commercial products. The electrolyte was made up of 0.5 M Na_2SO_4 + H_2SO_4 . The pH 3.50 and 4.50 values used in this work were adjusted to these figures by appropriate addition of H_2SO_4 or NaOH, respectively. $[P_2Mo_{18}O_{62}]^{6-}$ was prepared and characterized by one of the present authors [34]. In the present case of $[P_2Mo_{18}O_{62}]^{6-}$, the experiment was started, when necessary, with the two-electron reduced species.

The solutions were deaerated thoroughly for at least 1 h with pure argon and kept under a positive pressure of this gas during the experiments.

For work with gold electrodes, even though a pH 3.50 is suitable for the film deposition [18], pH 4.50 was selected to minimize the interference of proton reduction in the whole process.

The oxidized form of $[P_2Mo_{18}O_{62}]^{6-}$ is not stable at pH 4.50, but its two-electron reduced species is [35, 36]. Starting from this reduced species for our experiments has no deleterious consequences as the new films are expected to build up beyond the third wave of $[P_2Mo_{18}O_{62}]^{6-}$. Then, $[P_2Mo_{18}O_{62}]^{6-}$ is thoroughly reduced with 2F/mol in a pH 3.50 medium, and then the pH was adjusted to 4.50 for the subsequent work.

Results and discussion

From our preceding paper on this subject [18], several things have been learnt and will be recalled very briefly here, because they are useful to understand film deposition procedures. The electrochemistry of $[P_2Mo_{18}O_{62}]^{6-}$ has been described previously [18, 34, 35, 36]. In the pH domain where the anion is stable (pH $\leq$ 3.50), the first three waves feature two-electron reversible systems and showed no tendency to split into one-electron waves at high pH. Much the same results were found on a rotating platinum electrode in 1 M H_2SO_4 [36] and in cyclic voltammetry on a glassy carbon electrode [18] at pH 3.50. Electrodeposition of the new oxide film on the glassy carbon electrode surface became effective when more than six electrons were added to the starting molecule. From this obervation and others, it was concluded that the electrode derivatization should be faster if the less negative limit of the potential cycling domain were selected directly past the third wave of $[P_2Mo_{18}O_{62}]^{6-}$. The idea was successful. It appeared also that very low oxometalate concentrations are suitable for the electrodeposition.

The exact identity of the electrodeposited film is not known at present. Work is in progress by SEM and X-ray photoelectron spectroscopy (XPS) to approach the composition of the new metal oxide or mixture of metal oxides. Preliminary SEM results indicate that the Mo/P atomic ratio is much larger than that measured in the starting $[P_2Mo_{18}O_{62}]^{6-}$ molecule. Whether the phosphate moieties are linked to the deposited substance, or merely trapped in it, is still under investigation. Figure 1 shows a representative SEM image. It pertains to a rather thick film. The deposit is granular in nature. Similar images, with a far better resolution, have been obtained by atomic force microscopy (AFM) and confirm that the same kind of morphology is observed even at a very small scale. The results will be published elsewhere. Turning to the SEM images, we found that the whole surface is also homogeneously covered as the domain shown in the figure. XPS experiments reveal the presence of Mo^{VI} and Mo^{V} species. No particular care has been exercised, however, to protect the film from the dioxygen of air during the handling of the sample.

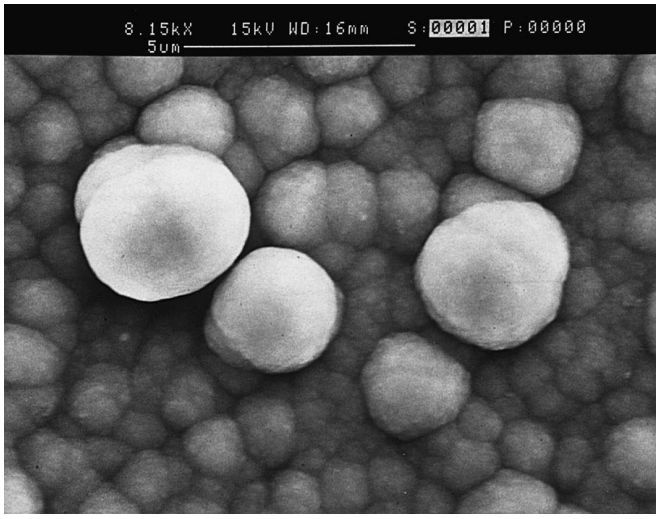

Fig. 1 A representative SEM image of a thick film electrodeposited from a two-electron-reduced solution of 1.6×10^{-4} M $[P_2Mo_{18}O_{62}]^{6-}$ + 0.5 M Na_2SO_4 (pH 4.50) on a highly oriented pyrolytic graphite electrode. For further details, see text

EQCM monitoring of film deposition from $[P_2Mo_{18}O_{62}]^{6-}$ on a gold electrode

As a preliminary step, it was necessary to study the electrochemical behaviour of $[P_2Mo_{18}O_{62}]^{6-}$ on a gold electrode. The EQCM configuration was chosen for this experiment. Figure 2A shows a representative cyclic voltammogram obtained for $[P_2Mo_{18}O_{62}]^{6-}$ at pH 3.50 with the gold electrode of the EQCM. The voltammetric pattern begins with three two-electron reversible waves as also observed previously [18, 36]. On the cathodic trace, a small peak appears after the third voltammetric wave. Generally, this peak is clearly seen during the second voltammetric cycle and grows on subsequent cycles. However, restriction of the negative potential limit just past the third voltammetric peak, reveals that the "small fourth peak" growing-up during potential cycles features a new product which might be one of the components of the new oxides to be deposited. All these observations are much the same as obtained previously on glassy carbon electrodes. Then, the study was begun with the potential domain restricted strictly to the first three waves of $[P_2Mo_{18}O_{62}]^{6-}$.

Figure 2B shows 15 consecutive records of the first three waves of $[P_2Mo_{18}O_{62}]^{6-}$ in the pH 3.50 medium used previously with glassy carbon. Here again, three well-behaved two-electron reversible systems are observed. In Fig. 2B are shown the first cyclic voltammogram and also those resulting from the continuous cycling of this pattern in the potential domain up to the third wave. Obviously, the whole cyclic voltammetric pattern does not change during this cycling. Thus, exactly as observed in the case of glassy carbon surfaces, no new material appears on the surface of the gold electrode, in the present experimental conditions.

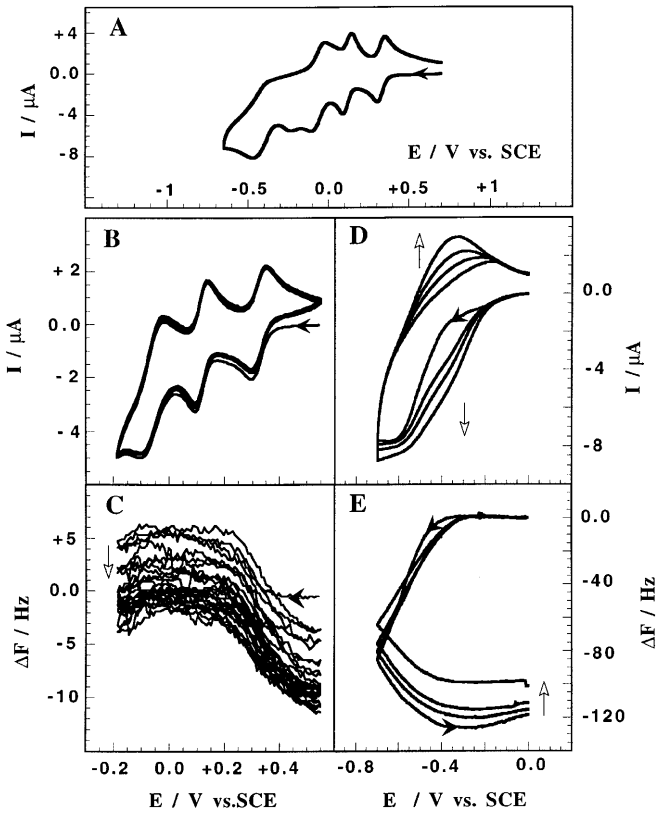

Fig. 2 **A** Representative cyclic voltammogram obtained on the gold electrode of the EQCM set-up, in a solution of 1.6×10^{-4} M $[P_2Mo_{18}O_{62}]^{6-}$ + 0.5 M Na_2SO_4 (pH 3.50). **B** Cyclic voltammetry pattern obtained upon continuous cycling of the gold electrode of the EQCM in a potential domain, restricted to the first three redox processes of $[P_2Mo_{18}O_{62}]^{6-}$. The solution is 1.6×10^{-4} M $[P_2Mo_{18}O_{62}]^{6-}$ + 0.5 M Na_2SO_4 (pH 3.50). **C** The EQCM frequency response corresponding to the voltammograms of **B**. **D** Selected representative cyclic voltammograms obtained on the gold electrode of the EQCM set-up during film electrodeposition from a two-electron reduced solution of 2×10^{-5} M $[P_2Mo_{18}O_{62}]^{6-}$ + 0.5 M Na_2SO_4 (pH 4.50). **E** EQCM frequency responses recorded simultaneously with the cyclic voltammograms of **D**. The scan rate is 10 mV/s. For further details, see text

Figure 2C represents the EQCM frequency responses recorded simultaneously with the cyclic voltammograms. The frequency variation corresponding to each cyclic voltammogram is small. Even the whole frequency shift during the continuous potential cycling is modest and seems to tend toward a limit, as indicated by the narrowing and then the superposition of the recorded traces. However, when the electrode potential is driven beyond the third voltammetric wave, an irreversible modification of the cyclic voltammogram is observed and is amplified on subsequent runs. In the following, we demonstrate that stable films can be obtained by a few discontinuous cycles. As a matter of fact, we found that a very few number of cycles already furnish fairly stable films.

Figure 2D shows a selected series of representative cyclic voltammograms run between 0 V and −0.7 V vs. SCE in a pH 4.50 sulfate medium. The potential starts from 0 V towards negative values to avoid oxidation of the two-electron reduced species of the heteropolyanion, but mainly because it is not expected to observe the "positive" waves of $[P_2Mo_{18}O_{62}]^{6-}$ when the appropriate films build up [18]. For the sake of clarity, only the first, third, fifth and the eighth voltammograms recorded discontinuously during an experiment are represented here. A slight current increase and a remarkable positive potential shift are observed for every other run. Another remark concerns the morphology of the waves. Their cathodic parts are clearly composite; this is less obvious for anodic traces, but they are large. In the cathodic pattern, at least two current components, which could also be composite themselves, are distinguishable. These voltammograms indicate that the film remains stable and continues to thicken at each run.

Figure 2E shows the EQCM frequency response recorded simultaneously with the voltammograms of Fig. 2D. The frequency decreases (mass increases) during the reduction step. This decrease slows down, but continues during the subsequent positive going scan. As a whole, the frequency variation observed during each cycle of the potential does not reverse to zero, even on maintaining the system in open circuit conditions. Because the EQCM frequency responses were culled from discontinuous potential cycling recording, these responses were reset at a common zero line. This observation indicates that some "irreversible" electrodeposition phenomenon is observed. Another feature in Fig. 1E deserves attention. Contrary to the current increase with time in Fig. 2D, the mass increase associated with each cyclic voltammogram decreases slightly after each other run, thus suggesting a slowing down of film thickness increase with time. Several phenomena could be invoked to explain the patterns observed on Figs. 2D and E. It is worth noting that the "first" cyclic voltammogram in Fig. 2D is rather "irreversible" and that reversibility gradually appears and is enhanced in the other runs. Even though the experimental conditions are clearly different, it must be pointed out that analogous behaviour had been observed during the continuous cycling in 1 M H_2SO_4 of WO_3 evaporated film electrodes containing a small amount of water and of WO_3 anodic film electrodes [37]. Also, as our electrode is still studied in the modification medium, electron exchange phenomena between the electrodeposited material and the molecules in solution must occur in parallel with the direct reduction/deposition of these molecules on the electrode surface. These phenomena could explain the current increase. Furthermore, the steady electrodeposition of the film and its own redox processes might be accompanied by a change in porosity with various consequences. Obviously, numerous processes could be operative. Therefore, further discussion is postponed until the electrodeposited film is studied in pure supporting electrolyte, which is more relevant to the present work.

This modified electrode is taken out from the modification medium, rinsed with the supporting electrolyte and transferred to this pure supporting electrolyte

(pH 4.50), for characterization. It is remarkable that the frequency measured with the film remains practically the same in the electrodeposition medium and after rinsing and transfer to the pure supporting electrolyte, thus confirming again the stability of the film. A surface wave is observed, which is also broad and composite. This surface wave could be cycled in the supporting electrolyte for a long period of time without any decrease.

Figure 3 summarizes the main findings: curves 1 and 1′ of this figure are respectively the last cyclic voltammogram in Fig. 2D and the corresponding EQCM frequency variation in Fig. 2E. Curves 2 and 2′ feature the surface wave observed in the pure supporting electrolyte and the associated EQCM frequency response. As expected, the surface wave is clearly smaller than the wave obtained in the modification medium. The difference is still more striking between the EQCM frequency responses reset at a common zero line. No significant admittance variation was measured between the experiments in the modification medium and in the pure supporting electrolyte. If Fig. 3A can be explained straightforwardly, Fig. 3B deserves more attention. Curve 2′ of Fig. 3B would indicate a modest but sizeable irreversible mass increase on the electrode surface.

Assuming that the rigid layer approximation holds for the the electrodeposited films, the apparent molar mass M of the deposited species can be evaluated. In these conditions, the frequency variation Δf is linearly related to the charge Q passed during the electrochemical process and the formula reads [22]:

$$\Delta f = \frac{10^6 M}{nF} \times K \times Q$$

where F is the Faraday constant, K is the calibration constant given in the Experimental section and n is the number of electrons transferred to effect the deposition. For the calculation, we assume two indicative values for n. With the present experimental conditions, the minimum value for n is $n = 6$. The second value will be taken as $n = 10$, following the remark that a four-electron wave is observed after the first three two-electron waves of $[P_2Mo_{18}O_{62}]^{6-}$ in 1 M H_2SO_4 [36]. This value should be considered as a reasonable guess, because possible disproportionation processes among the highly reduced species of $[P_2Mo_{18}O_{62}]^{6-}$ are not easy to take into account at present. With $Q = 108$ μC and $\Delta f = 101$ Hz, the evaluated values for M are 743 g and 1238 g for $n = 6$ and $n = 10$, respectively. The variation of Δf in the pure supporting electrolyte is only 8 Hz and has been neglected in the preceding calculation. The calculated values include the mass of the accompanying electrolyte and solvent. Even so, they are clearly lower than the molar mass of P_2Mo_{18} anion, which is 2780 g in the absence of neutralizing cations and in the absence of water molecules. The results indicate that some degradation of $[P_2Mo_{18}O_{62}]^{6-}$ occurs. However, MoO_3, with a molar mass of 144 g, cannot be the only species deposited. Thus, it appears likely that a partial decomposition of $[P_2Mo_{18}O_{62}]^{6-}$ will fit both with the evaluated masses and with the preliminary SEM results.

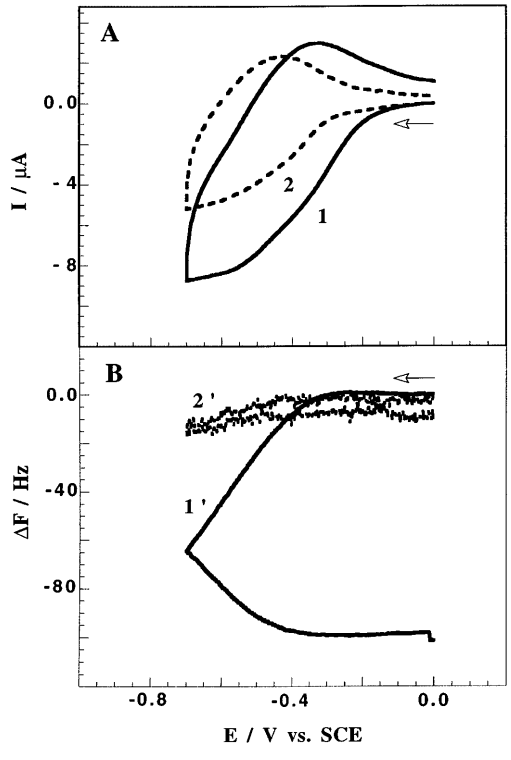

Fig. 3 Comparison of two cyclic voltammograms (**A**) and of the corresponding EQCM frequency responses (**B**). Scan rate: 10 mV/s. *Curve 1*: cyclic voltammogram corresponding to the eighth cycle of the electrode potential in a two-electron reduced solution of 2×10^{-5} M $[P_2Mo_{18}O_{62}]^{6-}$ in 0.5 M Na_2SO_4 (pH 4.50). *Curve 2*: the preceding modified electrode was taken out from the previous medium, and then cycled in the pure supporting electrolyte (pH 4.50)

EQCM characterization of the films electrodeposited from $[P_2Mo_{18}O_{62}]^{6-}$ solutions

In the pure supporting electrolyte, several striking observations are made. During a continuous potential cycling, the voltammogramm and the corresponding EQCM frequency response change steadily. Several series of such cycling experiments have been carried out successively. It must be pointed out that, at the end of each series, the modified electrode, left without polarization for several minutes to several hours in the supporting electrolyte, takes what can be termed an "equilibrium composition" in the medium. Then, the very first cyclic voltammogram at the beginning of a new series of potential cycling appears usually as slightly different from the subsequent ones as concerns its morphology and its potential location. In particular, its composite nature, the clear observation of which depends on the scan rate, is less marked than for subsequent ones. Figure 4A shows a typical first cyclic voltammogram at the beginning of a series of cycles. The corresponding EQCM response shows an "irreversible"

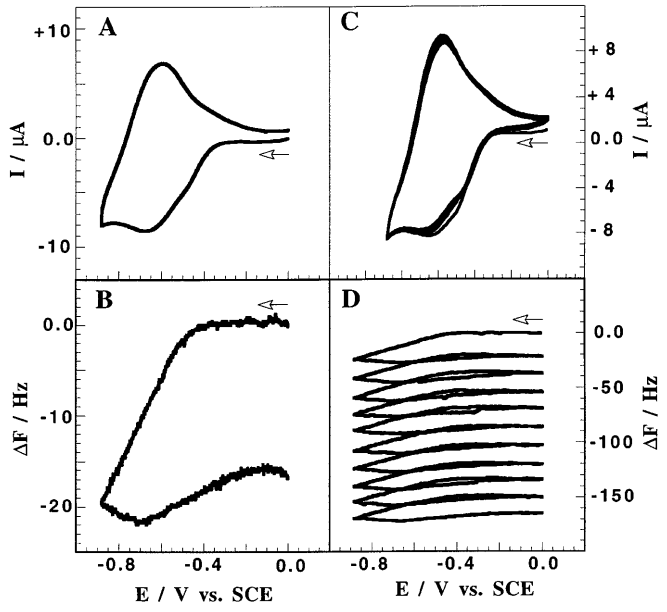

Fig. 4A–D Cyclic voltammograms obtained in the plain supporting electrolyte, 0.5 M Na_2SO_4 (pH 4.50) with an electrode modified as described in the text. Scan rate: 10 mV/s. **A** A representative cyclic voltammogram. **B** The EQCM frequency response associated with **A**. **C** Example of continuous cycling of a modified electrode. **D** The EQCM frequency response associated with **C**

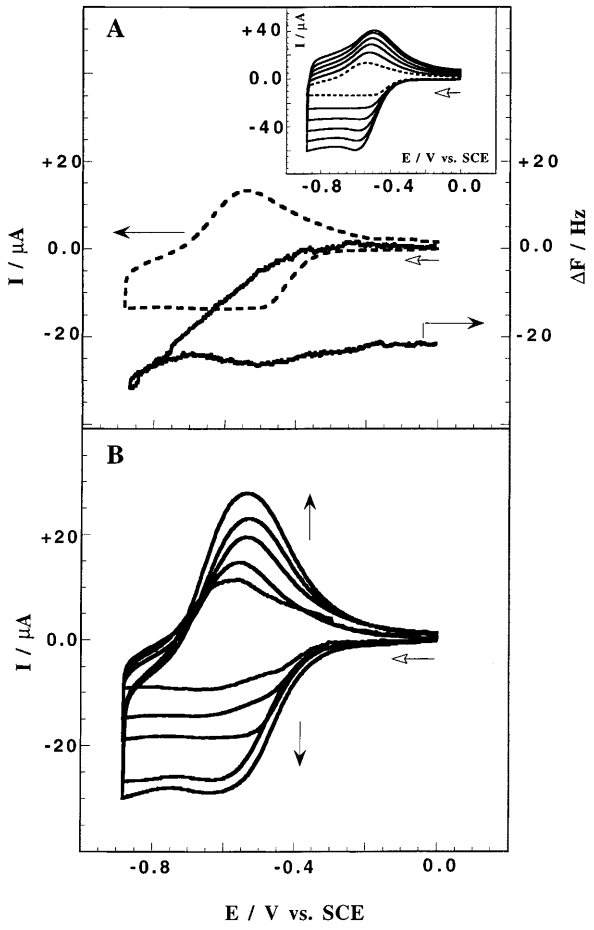

Fig. 5A, B Characteristic evolution of cyclic voltammograms with time. Scan rate: 10 mV/s. For other details, see text. **A** Example of cyclic voltammogram showing a polarogram-like plateau and the EQCM frequency response associated with it. *Inset*: evolution of the morphology of polarogram-like curves with scan rate. From the smallest to the highest currents, the scan rates are respectively: 10, 20, 30, 40, 50 and 60 mV/s. **B** A representative selection of cyclic voltammograms corresponding to increasing numbers of discontinuous cyclings of the same electrode

mass increase. This observation could appear surprising, as no heteropolyanion is available in the solution to induce eventually a film thickness increase. It is worth noting from Figs. 4A and B that this mass increase is correlated with the more cathodic of the two "waves" distinguishable in the composite trace in Fig. 4A. Figure 4C shows the cyclic voltammograms obtained during the continuous potential cycling initiated with Fig. 4A. Here again, a small but steady increase of the current is observed during the cycling. This increase concerns essentially the less cathodic part of the composite wave. The corresponding EQCM frequency response appears in Fig. 4D. It is worth pointing out that the irreversible mass increase is always larger at the end of the first scan than for subsequent ones. From the second scan onwards, the frequency decrease is much the same for each scan. This phenomenon has been observed for several tens of cycles and experiments. This indicates, at least, the long term permeability of the film.

In an attempt to elucidate the significance of the above observations, the cycling process was continued for several days, including rest periods. Figures 5 and 6 summarize the main information. The current function increases slowly but steadily for several days. One striking phenomenon is that the morphology of the cyclic voltammograms, in their cathodic traces, passes roughly from a one shoulder and one peak system to a single plateau-shaped wave and then again to a peak system. The particular case of the plateau current is shown in Fig. 5A, along with the corresponding EQCM frequency response. This simultaneous record of cyclic voltammetry and EQCM results confirms that the mass increase recorded by the EQCM actually begins at or just after the completion of the now "unique wave" of the composite system. In the inset of Fig. 5A, the influence of the scan rate has been studied on the evolution of the morphology of the cyclic voltammogram. In the inset, we start again from the plateau situation shown in Fig. 5A, at a scan rate of 10 mV/s (dotted line curve). It is observed that this situation persists at higher scan rates; however, the peak shape is gradually restored. The frequency responses show the following trend: the higher the scan rate, the smaller the "irreversible" part of mass increase. This behaviour remains whatever the wave shape. Figure 5B illustrates more generally the evolution of wave shapes as a function of time. It shows a representative selection of the last cyclic voltammograms obtained at the end of several series of continuous potential cycling programmes. The current increased with time during the cycling and also increased from one cycling session to the other. It is clear that the "two-

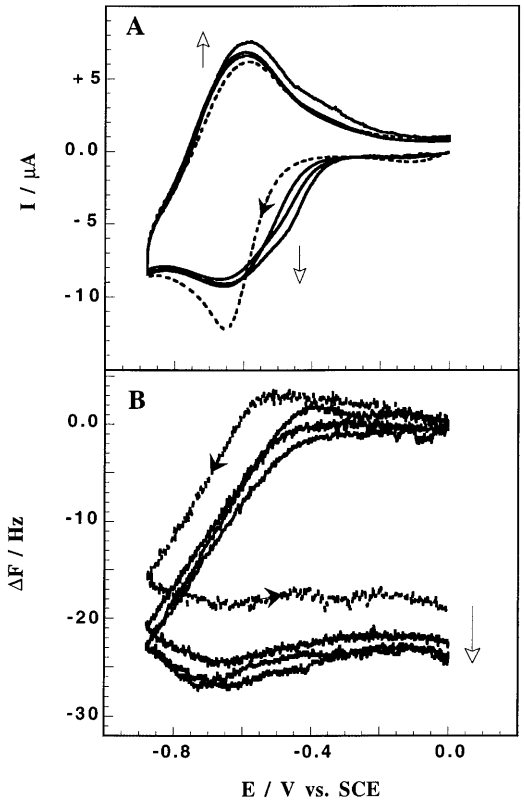

Fig. 6 **A** Evolution of cyclic voltammograms after several hours of rest of the modified electrode, without polarization in the pure supporting electrolyte of 0.5 M Na_2SO_4 (pH 4.50). The very first cyclic scan does not show any clear composite pattern (*dotted curve*). **B** The EQCM frequency responses corresponding to the above cyclic voltammograms. Scan rate: 10 mV/s

component'' composite wave gradually becomes a ''one-component'' plateau-shaped wave and then a ''one component'' peak-shaped wave.

Figure 6 illustrates also another influence of time. This influence is particularly striking with modified electrodes which have been cycled for a long period of time in the supporting electrolyte and that still show a cathodic composite wave ; however, the phenomenon remains true whatever the wave shape. The influence is described as follows: such an electrode is left without polarization, for at least several hours, and usually overnight, in the supporting electrolyte with a positive pressure of argon; then, the very first cyclic voltammogram recorded with this electrode shows a single ''normal-shaped'' pattern, with no apparent distorsion, as appears in Fig. 6A (dotted line). From the second potential scan onwards, the composite shape is restored with a continuous move in the positive potential direction. Concomitantly, the current ratio of the ''two components'' of the composite wave varies with time, the more positive one growing at the expense of the other. This evolution eventually ends in the observation of a single roughly plateau-shaped wave, at more positive potential than that observed in Fig. 6A (dotted line). The EQCM frequency responses in Fig. 6B indicate an important difference between the first scan and the others. However, from the second scan onwards, the observed frequency variations are comparable.

Some of the observed phenomena are not without analogous precedent in the pertinent literature [37–49]. For instance, during the continuous cycling in 1 M H_2SO_4 of a WO_3 evaporated film electrode [37], a steady current increase and an improvement in reversibility were observed and attributed to a continuous irreversible hydration of the film and a change in its porosity. Exactly as also observed in our experiments, the current increase is fast at the beginning and then slows down and reaches a maximum. However, after reaching this maximum, the current starts decreasing upon continuous cycling of the film of WO_3 [37]. Much the same indications appear in more recent papers [38–41], which emphasize also the influence of pH [39] or the role of irreversible trap sites in the films [40, 41]. By contrast, no such decrease was observed in the present work. It cannot be excluded that, despite a long but discontinuous cycling during several days, a situation likely to induce some degradation was still not reached. Also, an analogous irreversible cation and/or solvent uptake had been observed during the cycling of electrodeposited MoO_3 films [42, 43] and MoO_3 films prepared by thermal oxidation of electrodeposited MoS_3 [44]. As a whole, completely analogous explanations hold roughly for our observations. However, we note that the current intensity enhancement, the preservation of reversibility and the stability are much more remarkable in our system than in related ones [37–49]. We keep in mind that the method used to prepare the oxide films in the WO_3 as well as the MoO_3 series might lead to materials with different behaviour. However, the main electrochemical behaviour of our films and preliminary SEM and XPS results induce us to compare them more thoroughly with molybdenum oxide based films [42–49], including the existence of different trap sites in the films. It emerges out that the redox pattern of the films should feature intercalation/deintercalation processes, with irreversible water and/or electrolyte uptake up to maximum hydration. Before this maximum, the increase of the current between two successive series of potential cycling experiments indicates that part of the hydration, accompanied by a change in porosity, occurs during rest periods of the film. In this context, more or less complex molybdenum oxide bronzes are expected. The problem arises concerning the competition of hydrated proton and sodium cations for anionic sites in the film. As a matter of fact, pure sodium bronzes, pure hydrogen bronzes and mixed sodium and hydrogen bronzes are known in aqueous media [45].

In a different experiment, it has also been shown that the extent of lithium incorporation is negligible in MoO_3 films prepared by thermal oxidation of electrodeposited MoS_3 films and then cycled in 0.1 M $LiClO_4$, 14 mM $HClO_4$ and 2% H_2O/propylene carbonate [44]. This result indicates that the protons are the ionic species involved in the intercalation process, in this case [44].

Results culled from the literature [44, 45] indicate that the competition between hydrated protons and sodium ions should be actually active in the pH 4.50 solution used in our experiments. Our results might support these views. The observed composite reduction waves, for instance in Figs. 4–6 and the associated EQCM frequency responses, can be explained tentatively along these lines. In fact, much work, in several complementary directions, is still necessary before completely reliable interpretations of the observed phenomena could be given. Analysis of the films, at various stages of their synthesis or cycling, will be carried out. Also, the numerous possibilities of reduction of Mo(VI) species with associated chemical reactions should be considered [48]. One other very likely possibility is the existence of different insertion sites within the films [44, 49], which, associated with morphology changes, could explain the observed composite reduction waves. During several hours of rest periods, partial oxidation of the films by trace amounts of dioxygen might also intervene.

Finally, another fact should also be taken into account: it is indicated in the recent literature [50] that ammonium molybdophosphate irradiated with a large dose of electrons is partly converted to MoO_3 and ammonium molybdate. Here, it is worth reminding that we fix a large number of electrons on the skeleton of the heteropolyanion; furthermore, a pH 4.50 medium is used, and it is known that highly reduced species of $[P_2Mo_{18}O_{62}]^{6-}$ are not stable in acid media. Owing to these electrodeposition conditions used in our experiments, it is likely that a partial decomposition analogous to that described recently [50] is obtained. As a consequence, several "mixed" behaviours might be encountered. Then, the composite reduction might feature an association of the oxido-reduction of MoO_3 with waves of the starting or, presumably, a new heteropolyanion. The oxide, which can remain coated on the original salt [50], might bring about the properties of layered structures, useful for intercalation phenomena. Such a composition of the film might also explain several observed differences with other oxides described in the literature.

We found that the continuous cycling of the modified electrode in the potential domain from 0 V to −0.88 V ("cathodic pattern") favours the build-up of at least one species which could be oxidized at positive potential. In the following, this wave will be termed the "oxidation wave". Provisionally, it has been checked that the same behaviour is observed on glassy carbon electrodes and, therefore, cannot be ascribed to the use of Au film electrodes in the present experiments. Figure 7 illustrates this finding. The potential scanning program starts from zero to negative values, then goes to positive values before stopping at zero. As shown in Fig. 7A, the new main anodic wave in the positive potential domain is rather irreversible. After several strictly cathodic ($0\,V \rightarrow -0.88\,V \rightarrow 0\,V$) cycles, the oxidizable species is found to be stable, as suggested by the inset in Fig. 7A in which only the "oxidation wave" is scanned

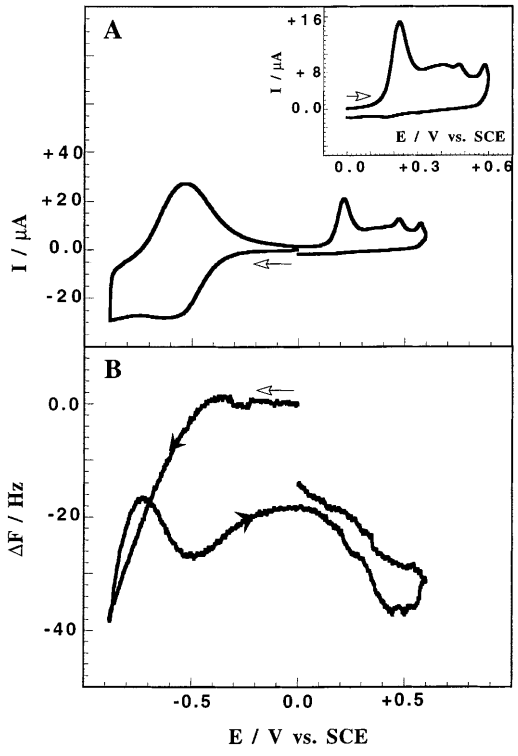

Fig. 7 **A** Complete cyclic voltammogram obtained in the pure supporting electrolyte of 0.5 M Na_2SO_4 (pH 4.50), with an electrode modified as described in the text and stabilized by a long cycling in the "cathodic domain"; the anodic domain is then explored and shows an irreversible oxidation pattern. Scan rate: 10 mV/s. For other details, see text. *Inset*: only the anodic wave is scanned. **B** The EQCM frequency responses corresponding to the complete cyclic voltammogram in **A**

($0\,V \rightarrow +0.6\,V \rightarrow 0\,V$). However, it must be pointed out that the current intensity of this wave decreases at every other scan, until it vanishes completely. Figure 7B shows the EQCM frequency response associated with the first whole potential scanning programme in Fig. 7A.

Other consequences of the scanning up to the "oxidation wave" appear on Fig. 8, showing a connection between this anodic wave and the "negative pattern". Only the negative potential domain is scanned. Curve 1 of Fig. 8A is merely the "negative pattern" of Fig. 7A. Curve 2 is the first cyclic voltrammogram ("negative pattern") obtained just after the whole potential scanning program ($0\,V \rightarrow -0.88\,V \rightarrow +0.6\,V \rightarrow 0\,V$) has been performed. The rather plateau-shaped cathodic wave now becomes peak-shaped with an overall negative shift in potential. A slight loss of reversibility is observed. From the second cyclic voltammetry run onwards (wave 3 of Fig. 8A), the plateau form is already visible and the initial pattern is completely restored upon the subsequent run. Incidentally, it must be noted that the "oxidation wave" (not shown) is fully restored after a larger number of cathodic scans. The EQCM frequency responses are interesting. Figure 8B, curve 2′, shows clearly that the film looses some species during the recording of curve 2 and that no irreversible intercala-

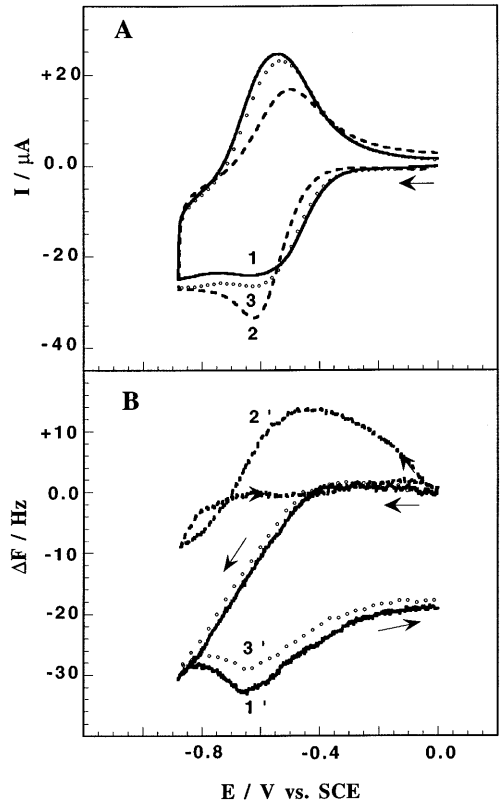

Fig. 8 **A** Cyclic voltammogram obtained in the pure supporting electrolyte of 0.5 M Na_2SO_4 (pH 4.50), with an electrode modified as described in the text and stabilized by a long cycling in the "cathodic domain". Scan rate: 10 mV/s. For other details, see text. *1* Cyclic voltammogram of the stabilized electrode, restricted to the cathodic domain, *2* First cyclic voltammogram restricted to the cathodic domain, obtained after the recording the oxidation pattern of Fig. 7A. *3* Second cyclic voltammogram restricted to the cathodic domain, obtained after the recording of the oxidation pattern. **B** The EQCM frequency responses corresponding to the above cyclic voltammograms

tion phenomenon is obtained, as no overall frequency variation could be observed at the end of the cycle. By contrast, the intercalation process is almost fully restored during the following scan (curve 3′, Fig. 8B). We propose the following rationale for these observations. Curves 2 and 2′ of Fig. 8 might be associated with a change in morphology or porosity of the film. As a matter of fact, we found that, when the film is oxidized and the potential returned to zero, the final mass is smaller than that obtained at the end of the cathodic scan, even though part of the irreversible insertion persists. This mass loss is believed to feature mainly a solvent and/or electrolyte egress. A shrinkage of the film should ensue. The phenomenon could explain the behaviour observed on curve 2′ of Fig. 8B, with no irreversible intercalation obtained during the first run following an oxidation process. An analogous change from intercalation to deintercalation during cyclic voltammetry has been observed recently [51] and attributed to the phase transformation of electrochemically precipitated nickel hydroxides.

All the preceding results make us assume that the present oxide film behaves much like layered materials of the MoO_3 and WO_3 series [37–49] Then, oxido-reduction phenomena observed in the "negative pattern" might feature also the dynamic intercalation/deintercalation processes of our new material. With such an hypothesis, previous work on MoO_3 [45] would suggest that a large ion like Cs^+ will not easily enter our new oxide material lattice, during potential cycling. Figure 9 illustrates the results of such an experiment. A film is first prepared in 0.5 M Na_2SO_4 (pH 4.50) and cycled in this medium up to "stabilization". The electrode is then taken out, rinsed with a Cs_2SO_4 solution adjusted to pH 4.50 with H_2SO_4, and then studied in this supporting electrolyte. The solid line curve of Fig. 9A is obtained. The new voltammetric pattern, which is the very first run in the presence of Cs^+, is clearly different from that observed in Na_2SO_4 medium (see, for instance, curve 1 of Fig. 8A). It is constituted by two well-separated cathodic waves. The less cathodic of them is small and

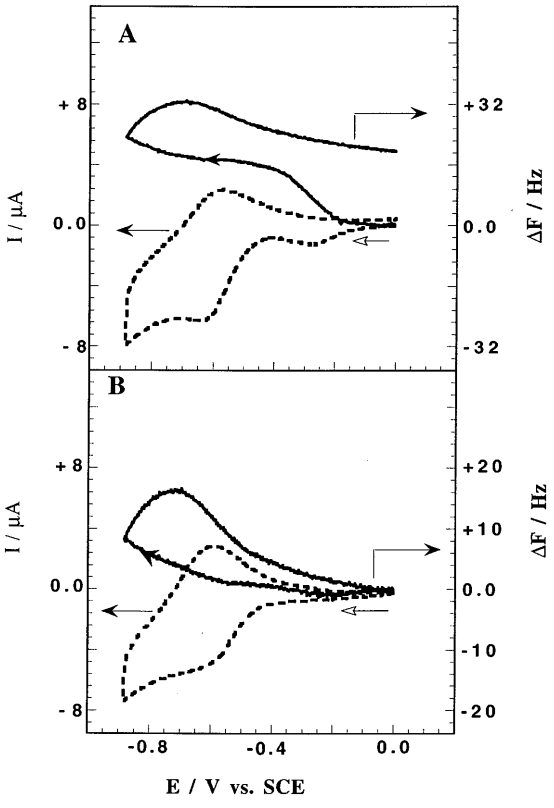

Fig. 9A, B Influence of Cs^+ cation on cyclic voltammograms and on the corresponding EQCM frequency responses. The modified electrode is prepared as previously and stabilized in the pure supporting electrolyte, 0.5 M Na_2SO_4 (pH 4.50). **A** The preceding electrode is taken out of the electrolyte, rinsed with the pure Cs_2SO_4 electrolyte and studied in Cs_2SO_4 solution (pH 4.50) with the same ionic strength as previous sodium solutions. The EQCM frequency response recorded simultaneously is superimposed on the cyclic voltammogram. **B** Evolution of the cyclic voltammogram and the corresponding EQCM frequency response during the cycling of the film in the Cs^+ supporting electrolyte. In **A** and **B**, attention is drawn to the directions of the frequency variations

apparently irreversible; the second one is the same as observed previously in the sodium medium, with a negative shift in potential. The EQCM frequency response (dotted line) is superimposed on the cyclic voltammogram. During all the negative going scan, an important loss of mass is observed, clearly at variance with the observation made in the presence of sodium. It must be noted that the mass loss continues partially during the subsequent positive going scan and that the frequency response does not reverse to its initial value at the end of this scan. Figure 9B shows the third voltammetric run and illustrates the evolution that takes place. The less cathodic of the voltammetric waves of Fig. 9A has disappeared and the second one has diminished slightly. The EQCM frequency response still features a steady mass loss during the negative going scan and part of the positive going one, but now the frequency reverses to its initial value at the end of the potential scan. On subsequent runs, the same pattern is repeated, with a continuous decrease of current as well as frequency amplitudes. All these observations would indicate that Cs^+ does not enter easily the new oxide lattice and is confined first in the very surface layer of the film. The less cathodic of the voltammetric waves in Fig. 9A should be associated with the presence of Cs^+. The difficulty of insertion of the cesium cation in the film during the time scale of our cyclic voltammetric runs would then explain the disappearance of the first cathodic wave and also the steady decrease of the second one during subsequent scans, leading gradually to a loss of electroactivity of the film. The current and frequency responses should also be associated with a change in morphology or porosity of the film. It must also be kept in mind that cesium salts of heteropolyanions are generally insoluble.

Conclusion

The reduction of $[P_2Mo_{18}O_{62}]^{6-}$ in mildly acidic aqueous media in the potential domain in which more than six electrons/molecule can be delivered to the heteropolyanion results in an electrodeposit which is then studied in pure supporting electrolyte. This film is adherent, persistent and electrochemically active. It has been possible to cycle the same sample several hundred times in the supporting electrolyte. An EQCM study of this system, in parallel with a more classical electrochemical study, when necessary, reveals several interesting behaviours of this film. A freshly deposited film shows a cyclic voltammetric pattern with two very closely spaced waves. The striking observation is a steady current increase and mass increase of this film during its continuous cycling in the pure supporting electrolyte. This behaviour was rationalized by considering the swelling of the film by continuous water and electrolyte uptake during redox processes of the film, up to a maximum, after which only intercalation/deintercalation processes are observed. It is worth mentioning that no tendency to dissolution has been observed for this film after several hundred cycles. We also emphasize the close analogy with WO_3 and MoO_3 bronzes, which suggests interpretations of the voltammetric and EQCM behaviours of the new metal oxides.

However, the wealth and variety of the observed behaviours demand that complementary work, in several directions, be carried out before a complete rationalization could be expected. For instance, study in progress might reveal remarkable electrochromic properties for the new materials. Also, from the study of Cs^+ cation, it is strongly suggested that ion effects should bring about several enlightening behaviours. Such studies are under way, along with the study of pH effects and solvent effects. In this context, intercalation/deintercalation of selected electroactive cations is envisioned. Also, work in progress by surface analysis and imaging techniques will help in determining the composition, the morphology of the film and related parameters.

Acknowledgement This work was supported by the CNRS and the Universities Paris XI and Paris VI. C. Severac (Métallurgie Structurale, Paris XI, Orsay), is thanked for preliminary XPS analyses.

References

1. Keita B, Nadjo L, Contant R, Fournier M, Hervé G (1989) Fr Patent (CNRS) 89/1728
2. Keita B, Nadjo L, Contant R, Fournier M, Hervé G (1990) Eur Patent (CNRS) Appl EP 382644; Chem Abstr (1991) 114: 191882
3. Keita B, Belhouari A, Nadjo L, Contant R (1995) J Electroanal Chem 381: 243
4. Toth JE, Anson FC (1989) J Am Chem Soc 111: 2444
5. Toth JE, Anson FC (1989) J Electroanal Chem 256: 361
6. Toth JE, Melton JD, Cabelli D, Bielski BHJ, Anson FC (1990) Inorg Chem 29: 1952
7. Sadakane M, Steckhan E (1998) Chem Rev 98: 219
8. Keita B, Nadjo L (1989) Mater Chem Phys 22: 77
9. Keita B, Nadjo L (1993) Curr Top Electrochem 2: 77
10. Keita B, Nadjo L, Parsons R (1989) J Electroanal Chem 258: 207
11. Keita B, Nadjo L (1993) J Electroanal Chem 354: 295
12. Keita B, Nadjo L (1985) J Electroanal Chem 191: 441
13. Keita B, Nadjo L (1988) J Electroanal Chem 243: 87
14. Keita B, Nadjo L (1990) J Electroanal Chem 287: 149
15. Belhouari A, Keita B, Nadjo L, Contant R (1998) New J Chem p 83
16. Contant R, Abbessi M, Canny J, Belhouari A, Keita B, Nadjo L (1997) Inorg Chem 36: 4961
17. Keita B, Nadjo L (1988) J Electroanal Chem 247: 157
18. Keita B, Nadjo L, Contant R (1998) J Electroanal Chem 443: 168
19. Wolff CM, Schwing JP (1976) Bull Soc Chim Fr 679: 675
20. Lahr SK, Finklea HO, Schultz FA (1984) J Electroanal Chem 163: 237
21. Kulesza PJ, Faulkner LR (1988) J Am Chem Soc 110: 4905
22. Buttry DA (1991) In: Bard AJ (ed) Electroanalytical chemistry, vol 17. Dekker, New York, p 3
23. Keita B, Nadjo L, Bélanger D, Wilde CP, Hilaire M (1995) J Electroanal Chem 384: 155
24. Kuhn A, Anson FC (1996) Langmuir 12: 5481
25. Launay JP (1972) Thesis. University Paris VI
26. Izumi Y, Hasebe R, Urabe K (1983) J Catal 84: 402

27. Ai M (1981) J Catal 71: 88
28. Kasztelan S, Payen E, Moffat JB (1988) J Catal 112: 320
29. Rocchiccioli-Deltcheff C, Amirouche M, Fournier M (1992) J Catal 138: 445
30. Keita B, Nadjo L (1993) J Electroanal Chem 354: 295
31. Rong C, Anson FC (1994) Anal Chem 66: 3124
32. Schwegler MA, Vinke P, Vander Eijik M, Van Bekkum H (1992) Appl Catal A80: 41
33. Castillo MA, Vazquez PG, Blanco MN, Caceres CV (1996) J Chem Soc Faraday Trans 92: 3239
34. Ciabrini JP, Contant R, Fruchart RM (1983) Polyhedron 2: 1229
35. Souchay P, Contant R, Fruchart JM (1967) CR Acad Sci Paris 264: 976
36. Papaconstantinou E, Pope MT (1967) Inorg Chem 6: 1152
37. Reichman B, Bard AJ (1979) J Electrochem Soc 126: 583
38. Babinec SJ (1992) Sol Energy Mater Sol Cells 25: 269
39. Ogura K, Nakayama M, Endo N (1998) Electroanal Chem 451: 219
40. Kim D-J, Pyun S-I, Choi Y-M (1998) Solid State Ionics 109: 81
41. Kim D-J, Pyun S-I (1998) Electrchim Acta 46: 2341
42. Guerfi A, Dao LH (1989) J Electrochem Soc 136: 2435
43. Guerfi A, Paynter RW, Dao LH (1995) J Electrochem Soc 142: 3457
44. Laperriere G, Lavoie MA, Bélanger D (1996) J Electrochem Soc 143: 3109
45. Schöllhorn R, Kuhlmann R, Besenhard JO (1976) Matet Res Bull 11: 83
46. Baba N, Morisaki S, Nishiyama N (1984) Jpn J Appl Phys 23: L638
47. Anbananthan N, Rao KN, Venkatevan VK (1994) J Electroanal Chem 374: 207
48. Gorenstein A, Scarminio J, Lourençao A (1996) Solid State Ionics 86–88: 977
49. Yu A, Kumagai N, Liu Z, Lee JY (1998) Solid State Ionics 106: 11
50. Narasimharao KL, Sarma KS, Mathew C, Jadhav AV, Shukla JP, Natarajan V, Seshagiri TK, Sali SK, Dhiwar VI, Pande B, Venkataramani B (1998) J Chem Soc Faraday Trans 94: 1641
51. Kim MS, Kim KB (1998) J Electrochem Soc 145: 507